analytical chemistry

Article

pubs.acs.org/ac

Development of a GC/Quadrupole-Orbitrap Mass Spectrometer, Part I: Design and Characterization

Amelia C. Peterson,[†] Jan-Peter Hauschild,[⊗] Scott T. Quarmby,[○] Dirk Krumwiede,[⊗] Oliver Lange,[⊗] Rachelle A. S. Lemke,[§] Florian Grosse-Coosmann,[⊗] Stevan Horning,[⊗] Timothy J. Donohue,[§,⊥] Michael S. Westphall,[∥] Joshua J. Coon,*[,†,‡,∥] and Jens Griep-Raming[⊗]

[†]Departments of Chemistry, [‡]Biomolecular Chemistry, and [§]Bacteriology, University of Wisconsin−Madison, Madison, Wisconsin 53706, United States

[∥]Genome Center of Wisconsin, Madison, Wisconsin 53706, United States

[⊥]Great Lakes Bioenergy Research Center, Madison, Wisconsin 53703, United States

[⊗]Thermo Fisher Scientific, 28199, Bremen, Germany

[○]Thermo Fisher Scientific, Austin, Texas 78728, United States

Supporting Information

ABSTRACT: Identification of unknown compounds is of critical importance in GC/MS applications (metabolomics, environmental toxin identification, sports doping, petroleomics, and biofuel analysis, among many others) and remains a technological challenge. Derivation of elemental composition is the first step to determining the identity of an unknown compound by MS, for which high accuracy mass and isotopomer distribution measurements are critical. Here, we report on the development of a dedicated, applications-grade GC/MS employing an Orbitrap mass analyzer, the GC/Quadrupole-Orbitrap. Built from the basis of the benchtop Orbitrap LC/MS, the GC/Quadrupole-Orbitrap maintains the performance characteristics of the Orbitrap, enables quadrupole-based isolation for sensitive analyte detection, and includes numerous analysis modalities to facilitate structural elucidation. We detail the design and construction of the instrument, discuss its key figures-of-merit, and demonstrate its performance for the characterization of unknown compounds and environmental toxins.

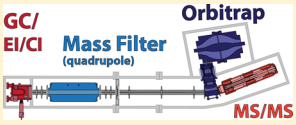

The success of small molecule analysis, especially metabolomics, by gas chromatography/mass spectrometry (GC/MS) hinges on the ability to chemically identify, through elemental composition annotation and structural characterization, the compounds in unknown peaks.[1] As a mature analytical technique, sample analysis workflows and post-processing methods for GC/MS are well-established. Nonetheless, in a single GC/MS analysis of a complex sample, often only ∼100 of the 200−500 observed mass spectral features can routinely be identified;[1−4] the rest remain unknown, along with their potential importance to the research question being studied.

The first step to identifying an unknown is elemental composition derivation, where high mass accuracy is important[5] but not sufficient.[6] Fiehn has shown that a simple two-step approach of (1) calculation of candidate compositions from the mass and (2) elimination of false candidates by comparison of empirical and theoretical isotopomer distributions is a highly effective tool to determine elemental compositions from high mass accuracy data.[6,7] Thus, as the GC/MS field is tasked with the analysis of complex biological and environmental samples containing multitudinous unknowns, the demand and necessity for state-of-the-art, high resolution and high mass accuracy instrumentation has grown.

Despite the high impact the Orbitrap analyzer has had in proteomics, and liquid chromatography/mass spectrometry (LC/MS) in general, no Orbitrap-based system dedicated to GC/MS has been developed. Recently, we reported on a proof-of-principle modification of an electron transfer dissociation-enabled quadrupole linear ion trap (QLT)-Orbitrap[8] for GC/MS to assess the merits of the Orbitrap as a detector for GC.[9] Despite the numerous drawbacks and crude design of this implementation, the performance of this proof-of-principle system nonetheless suggested that a purpose-built and optimized GC/Orbitrap instrument could serve several demanding applications in GC/MS-based fields, especially in fields like metabolomics that rely on the unambiguous identification of unknowns.[1,7,10]

Here, we introduce an Orbitrap for GC applications, the GC/Quadrupole-Orbitrap, which substantially improves upon the proof-of-principle system: using a benchtop Orbitrap LC/MS[11,12] as the base platform, we have developed an applications-grade GC/MS that not only enables high mass accuracy and high resolution analysis, but does so at scan rates amenable to the time-scale of GC separations. The GC/Quadrupole-Orbitrap can be used for a range of applications from trace analysis to the structural characterization of unknown metabolites in metabolomic analyses. Additionally,

Received: March 26, 2014
Accepted: August 18, 2014
Published: August 19, 2014

   dx.doi.org/10.1021/ac5014767 | *Anal. Chem.* 2014, 86, 10036−10043

we have developed an advanced data-dependent acquisition algorithm for MS/MS of alkylsilylated analytes, molecular ion-directed acquisition (MIDA), which is detailed in the accompanying article.[13] Herein, we discuss the design and construction of the instrument, detail optimization of the hardware, electronics, and firmware, and benchmark instrument figures-of-merit.

EXPERIMENTAL SECTION

Reagents. Unless otherwise specified, all reagents were purchased from Sigma-Aldrich (St. Louis, MO). Methanol and water (Optima LC/MS grade), and pyridine, methylene chloride, and iso-octane (GC/pesticide grade) were purchased from Fisher Scientific (Fair Lawn, NJ). Compressed gases (methane, helium, and nitrogen) were ultrahigh purity grade and purchased from Airgas (Madison, WI).

Sample Preparation and Gas Chromatography/Mass Spectrometry. GC/MS experiments were performed on a Trace GC Ultra gas chromatograph (Thermo Fisher Scientific, Milan, Italy) equipped with a GC PAL autosampler (CTC Analytics, Zwingen, Switzerland). Compounds were separated on a 30 m × 0.25 mm (i.d.) × 0.25 μm (d_f) Crossbond 5% diphenyl/95% dimethyl polysiloxane column (Restek Rxi-5Sil MS, Bellefonte, PA) with He carrier gas. The GC was interfaced to the Quadrupole-Orbitrap instrument via a heated transfer line. The instrument was characterized and regularly tuned and calibrated with perfluorotributylamine (FC-43; Scientific Instrument Services, Ringoes, NJ), introduced into the transfer line by a calibration gas module. All MS experiments employed automatic gain control (AGC)[12,14,15] and advanced signal processing (ASP),[16−19] and were acquired in profile mode.

Octafluoronaphthalene. Solutions of 1 pg/μL octafluoronaphthalene (OFN) were prepared in iso-octane containing 0%, 1%, 2%, and 5% (v/v) diesel fuel, obtained from a local gas station. Aliquots (1 μL) were analyzed in triplicate, splitless, via the hot-needle technique at an injector temperature of 220 °C and separated at 1.2 mL/min He with oven gradient: isothermal at 40 °C for 1 min, 30 °C/min to 165 °C, 120 °C/min to 275 °C, and isothermal at 275 °C for 5 min. The transfer line and source temperatures were 275 and 220 °C, respectively. The MS was configured for single ion monitoring (SIM), using a 5 Th window around the OFN monoisotopic peak (m/z 272), a scan range of m/z 106−300, resolution of 70 000 ($m/\Delta m$), relative to m/z 200, maximum injection time of 250 ms, and AGC target of 1×10^6. Electron ionization (EI, 70 eV) was used.

EPA 8270 Pesticides Analysis. A 25−50 μg/mL working solution in methylene chloride of 93 EPA 8270 semivolatile organic pollutants was prepared by combination of the following, all obtained from Restek: SV Internal Standard Mix, Benzoic Acid Mix, Revised B/N Surrogate Mix, 8270 Benzidines Mix No. 2, 1,4-dioxane, 8270 MegaMix, and Acid Surrogate Mix (4/89 SOW). The working solution was serially diluted from 25−50 μg/mL (2.5−5 ng on column) to 25−50 pg/mL (2.5−5 fg on column) in methylene chloride. A volume of 1 μL each was analyzed in triplicate using EI (70 eV) at an injection split ratio of 10:1 and 1.2 mL/min He column flow. The following oven program was used: 1 min isothermal at 80 °C, 25 °C/min to 280 °C, 5 °C/min to 320 °C, and 1 min isothermal at 320 °C. The injector, transfer line, and source temperatures were 270, 280, and 250 °C, respectively. Targeted SIM analyses targeted the monoisotopic peak, or most-abundant ion, of 93 pesticides with 3 Th isolation windows based on a scheduled inclusion list (Supplemental Table S1 in the Supporting Information), with a resolution of 17 500, an AGC target of 1×10^6, and maximum injection time of 100 ms.

Polychlorinated Dibenzo-p-Dioxin and Dibenzofuran Analysis. Intrarun sensitivity, linearity, and response reproducibility for tetrachlorodibenzo-*p*-dioxins (TCDD) was quantified with two standard mixtures of 6 TCDD congeners (Campro Scientific, Berlin, Germany) at concentrations ranging from 2 to 100 fg/μL, or each at 10 fg/μL, respectively. Native and ^{13}C-labeled internal standard congeners were analyzed in targeted SIM mode with 10 Th windows using EI (70 eV), 300 μA emission current, 250 ms maximum injection time, and resolution 17 500. An extract of pooled human blood containing tetra- and hexachlorodibenzo-*p*-dioxin and hexachlorodibenzofuran congeners previously quantified at ∼10−15 fg/uL using magnetic sector instrumentation and standard methods conforming to EPA 1613 was provided by Thermo Fisher Scientific (Bremen, Germany). The sample was analyzed in targeted SIM mode with 2 Th windows for native congeners and full scan mode for internal standards (at 1 pg/μL). Other parameters were the same as for the standard TCDD mixtures.

Structural Characterization of an Unknown Fatty Acid Methyl Ester (FAME). Bacterial fatty acids were methyl esterified using sodium methoxide in anhydrous methanol at RT for 2 h. The reaction was quenched with 2 N HCl and FAMEs were extracted with hexane. For hydrogenation experiments, extracted FAMEs were dried under nitrogen and subsequently hydrogenated in chloroform/methanol (2:1 v/v) with 5% Pt on charcoal as detailed by Montanari et al.[20] A bacterial acid methyl ester (BAME) mix standard, containing 26 FAMEs in methyl caproate, was used for system optimization. Samples in hexane (1 μL) were injected via the hot-needle technique at various split ratios depending on sample concentration, with an injector temperature of 250 °C, He flow rate of 1 mL/min, and the following oven program: 1 min isothermal at 150 °C, 15 °C/min to 250 °C, 1 min isothermal at 250 °C, 80 °C/min to 320 °C, and 2 min isothermal at 320 °C. The transfer line and source temperatures were 280 and 250 °C, respectively. Samples were ionized via EI or positive mode chemical ionization (CI/PCI) using acetonitrile (ACN) as the reagent gas (70 eV). Full-scan analyses employed a scan range of m/z 75−400, resolution of 17 500, AGC target of 1×10^6, and maximum injection time of 100 ms. Targeted MS/MS analyses employed a 5 Th isolation window, normalized collision energy of 25 eV, resolution of 17 500, AGC target of 1×10^6, and maximum injection time of 250 ms.

For ACN PCI, 250 μm (i.d.) fused silica capillary connected an ACN reservoir (6 mL) directly to the MS source through the transfer line. A two-holed ferrule permitted entry of both GC column and ACN capillary into the transfer line. While the column extended into the source, the ACN capillary was set back ∼5 cm from the source to prevent interference with the GC eluent. A medium-flow metering valve (Swagelok, Solon, OH) between the reservoir and transfer line regulated the flow of ACN into the source. A source pressure of 7.1×10^{-5} Torr, ∼0.2 ms reagent injection time (at a 1×10^6 AGC target), and m/z 42 (protonated ACN)-to-m/z 54 (1-methyleneimino-1-ethenylium, or MIE) ratio of 5:1 were optimal for generation of molecular ion MIE-adducts of unsaturated FAMEs.

Analysis of Arabidopsis thaliana Polar Extracts. Polar metabolite extracts of *A. thaliana* were prepared and analyzed as detailed in the accompanying article.[13] Briefly, wild-type *A.*

dx.doi.org/10.1021/ac5014767 | Anal. Chem. 2014, 86, 10036−10043

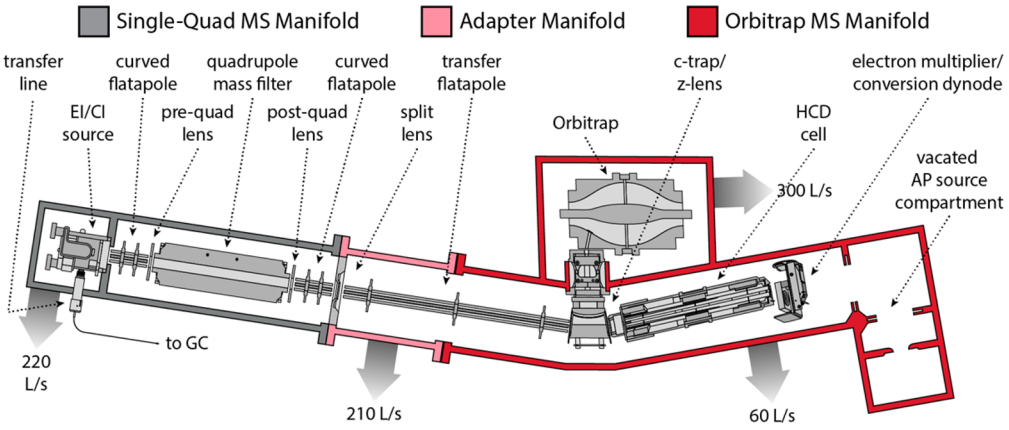

Figure 1. Schematic of the GC/Quadrupole-Orbitrap instrument. The three component manifolds, the Single-Quadrupole MS, adapter, and Exactive, are colored in gray, light red, and dark red, respectively. The main ion optic components and four turbo-molecular pumps (as gray outward arrows) are labeled.

thaliana were grown in liquid culture in stable isotope-enriched media ($^{12}C^{14}N$, $^{12}C^{15}N$, $^{13}C^{14}N$, and $^{13}C^{15}N$). Following 12 d growth, plants were harvested, flash frozen, and macerated to a fine powder. Aliquots of ~250−350 mg of powder were extracted as reported by Fiehn,[21] and polar fractions subjected to methoxyamination and silylation with either *N*-(*t*-butyldimethylsilyl)-*N*-methyltrifluoroacetamide (MTBSTFA) or *N*-methyl-*N*-(trimethylsilyl) trifluoroacetamide (MSTFA) (Thermo Scientific, Bellafonte, PA). Samples were ionized with either EI or methane PCI using full scan MS or molecular-ion directed acquisition (MIDA)-MS/MS.

Data Analysis. Data were both manually queried and automatically processed within Xcalibur Qual Browser 2.3 (Thermo Fisher Scientific). Unless otherwise indicated, data were extracted with ±5−10 ppm mass error tolerances and peak areas (area-under-the-curve, AUC) determined via the ICIS peak detection algorithm. Regression and statistical analyses were performed in Origin (version 8.5.1 SR2, Origin Lab, Northampton, MA). Isotopomer abundance or ratio errors were calculated from the theoretical isotopomer abundances expected for a given elemental formula. For EPA 8270 pesticide analysis, the ratio of first isotopomer to the sum of the monoisotopomer and first isotopomer abundances was used. For *Arabidopsis thaliana* metabolomic analysis, the percent errors of the abundances of the first, second, and third isotopomers relative to the monoisotopomer abundance were used, conforming to the standard used by the Seven Golden Rules Excel macro.[7,13]

RESULTS AND DISCUSSION

Instrument Construction. The GC/Quadrupole (Q)-Orbitrap MS instrument consists of a single-quadrupole GC/MS (DSQ II; Thermo Fisher Scientific, Austin, TX) and a benchtop Orbitrap MS (Exactive; Thermo Fisher Scientific, Bremen, Germany) coupled together via an adapter manifold, shown in Figure 1 in gray, dark red, and light red, respectively. Construction proceeded by removing the Orbitrap MS's atmospheric pressure (AP) inlet and associated ion optics and sealing the AP inlet manifold openings with custom flanges. The two-stage source turbo-molecular pump was then removed and replaced with a smaller, turbo-molecular pump (60 L/s; Pfeiffer Vacuum, Asslar, Germany) to reflect the decreased pumping requirements. Into this vacated space, the beam-type CAD (collisional activation and dissociation) collision cell (higher energy CAD, or HCD, cell, for MS/MS) and electron multiplier/conversion dynode (EM) were relocated from the opposite side of the Orbitrap MS's c-trap and from the single-quadrupole MS, respectively. Connections for the EM to the external electrometer and dynode power supply were made via a custom top-flange. On the opposite side of the Orbitrap MS's c-trap, the adapter manifold joined the single-quadrupole MS manifold to the manifold previously housing the HCD cell. The EI/CI combination source, curved prefilter flatapole, pre-quadrupole lens, and quadrupole mass filter of the single-quadrupole MS remained. The gap between the quadrupole mass filter and the c-trap of the Orbitrap MS was bridged by the addition of a post-quadrupole lens, curved flatapole, custom split lens for ion gating, and long transfer flatapole. The adapter manifold was fitted with a turbo-molecular pump (210 L/s; Pfeiffer Vacuum). Electrical connections for the additional ion optics elements were made by feed-throughs installed in the adapter manifold. The HCD cell was plumbed directly with ultrahigh purity nitrogen collision gas, which also provided collisional cooling in the attached c-trap. The EI/CI source was interfaced to the GC via a heated transfer line. All component parts are labeled in Figure 1.

Electronics and Firmware Modifications. Most of the original electronics from both instruments were retained to drive original and new ion optic and vacuum components. The EI/CI source elements and the EM remained under single-quadrupole MS electronic control, except for EI/CI source lens 2 (see Supplemental Figure S1 in the Supporting Information). Control of source lens 2 was redirected to a spare dc output on the Orbitrap MS. The Orbitrap MS electronics retained control over the same components, as well as additional single-quadrupole MS components and all new ion optic devices. The Orbitrap MS rf and dc outputs, originally controlling AP inlet devices, were repurposed to drive the curved flatapoles and pre/post-quadrupole mass filter lenses. The split lens electronics were modified to provide an ion deflection potential of ±50 V, rather than ±350 V, and to drive the new split lens device. Two new circuit boards were added to the system to control the quadrupole mass filter and provide rf and dc control for the transfer flatapole.

The Orbitrap MS instrument firmware (written in Python and based on Thermo Q Exactive firmware version 2.0) was adapted to permit simultaneous control of both component instruments via a single data system. Code was written to

dx.doi.org/10.1021/ac5014767 | *Anal. Chem.* 2014, 86, 10036−10043

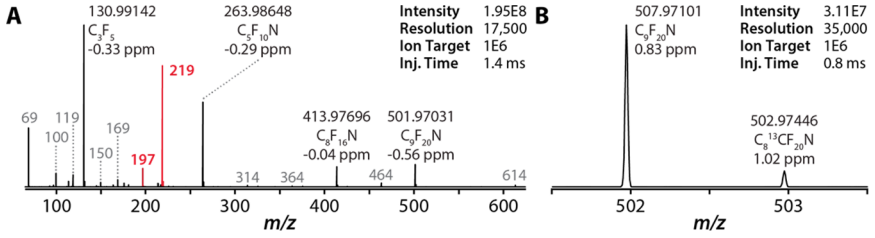

Figure 2. (A) Single-scan full mass range positive EI FC-43 calibration spectrum acquired in profile mode. Mass errors (ppm) and compositions are shown for major ion species. Average mass error with external calibration was 0.24 ppm (σ = 1.04, $error_{rms}$ = 1.06, n = 38). Mass accuracy and compositions for additional ions are available in Table S2 in the Supporting Information. (B) Zoom-in on FC-43 m/z 502 monoisotope and first isotope acquired at 35 000 resolution in profile mode.

enable ion injection, automatic gain control (AGC), manual and automated signal optimization, ion optic and mass analyzer calibration, quadrupole isolation, and MS/MS capabilities.

Scan Rate and Resolution. Scan rates vary as a function of resolution, and range from 24.1 Hz at resolution 8 500 down to 1.0 Hz at resolution 200 000 (see Supplemental Figure S2 in the Supporting Information). Ion injection and mass analysis parallelization can be employed up to resolution 130 000 (512 ms transient). If one considers a scan rate of 4 Hz to be the absolute minimum for practical application of this technology on GC-time scale, the GC/Q-Orbitrap is amenable to analyses requiring resolution up to 100 000.

Spectral Figures-of-Merit and Quality. The FC-43 calibration spectrum provides insight into several figures-of-merit and serves as the basis for all calibration procedures (e.g., calibration of ion transmission, mass accuracy, analyzer injection, advanced signal processing (ASP), and quadrupole isolation). First, the single-scan FC-43 profile spectra in Figure 2A,B highlight the instrument's typical mass accuracy and precision, demonstrating externally calibrated mean mass errors of 0.24 ± 1.04 ppm for 38 routinely observed ions ($error_{rms}$ = 1.06 ppm) (Supplemental Table S2 in the Supporting Information). Second, routine 1−2 ms ion accumulation times at an AGC target of 1 × 10^6 indicate the overall efficiency of the generation and transmission of ions. Third, a full distribution of ions spanning the mass range from m/z 69−614 with significant representation of fragile or reactive ions (m/z 219, m/z 502, and m/z 614) attests to the "gentleness" of the injection path, the absence of unexpected mass discrimination issues, and low levels of background water vapor (a 3:1 ratio of m/z 219:197 is typical for GC-trapping instruments).

While these specifications are tailored to the FC-43 calibration spectrum (Supplemental Figure S3 in the Supporting Information), spectra collected on an instrument that is calibrated to minimize ion/molecule reactions, mass discrimination, and the harshness of ion transmission should similarly demonstrate little evidence of those adverse effects in analyte spectra. In GC/MS, the primary method of chromatographic feature annotation is to match experimental spectra against large reference databases of EI spectra.[22] As such, spectra quality is dictated by the extent of the match between experimental and reference spectra. In Figure 3, experimental single-scan spectra of methyl eicosanoate (C20:0, $C_{21}H_{42}O_2$) (panel A) and hexachloroethane (C_2Cl_6) (panel B) are juxtaposed with unit-resolution reference spectra from the NIST database[22] (in red). Both experimental spectra faithfully reproduce the expected ions and relative abundances present in the reference spectra and are correctly matched as the top hit by NIST with match scores of 85.3 and 95.0, respectively. The slight left- or right-shift of the experimental spectra is due to

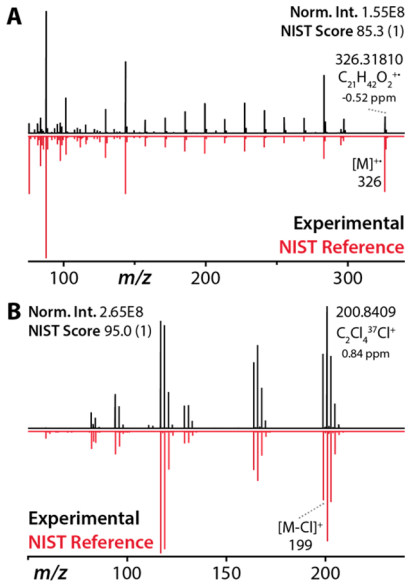

Figure 3. Spectral quality of GC/Q-Orbitrap spectra (top, black) for (A) methyl eicosanoate (average mass error 0.57 ppm, σ = 0.50 ppm, $error_{rms}$ = 0.75 ppm, n = 16) and (B) hexachloroethane (average mass error 1.14 ppm, σ = 0.39 ppm, $error_{rms}$ = 1.19 ppm, n = 7). Spectra are juxtaposed with NIST reference spectra (bottom, red). Spectra were matched as the top hit (number in parenthesis) with NIST match scores as indicated. Spectra were acquired at 17 500 resolution with a 1 × 10^6 ion target.

mass defects that are missing in the library spectra because of peak centroiding to the nearest nominal mass and unit-mass accuracy mass analysis. The GC/Q-Orbitrap spectra possess, in these two examples, an average mass error of 0.57 ± 0.50 ppm and 1.14 ± 0.39 ppm, respectively. High mass accuracy and retention of all spectral features (i.e., the mass defect) facilitate elemental composition assignment and identification, even in the absence of library spectra.

Quadrupole Isolation. A quadrupole mass filter was included in the GC/Q-Orbitrap design to boost instrument sensitivity in targeted and trace analyses, used in experiments such as targeted selected ion monitoring (SIM), targeted MS/MS, or data-dependent MS/MS. While both SIM and MS/MS improve sensitivity for target analytes under high background conditions by enhancing analyte signal-to-noise, the latter also facilitates target identification and structural elucidation. For the purpose of enhancing S/N in trace analyses, two competing processes must be reconciled. First, to accumulate greater populations of ions the target analyte must be efficiently transmitted through the quadrupole, with wider isolation widths yielding higher transmission efficiency.[23] Second, to

dx.doi.org/10.1021/ac5014767 | Anal. Chem. 2014, 86, 10036−10043

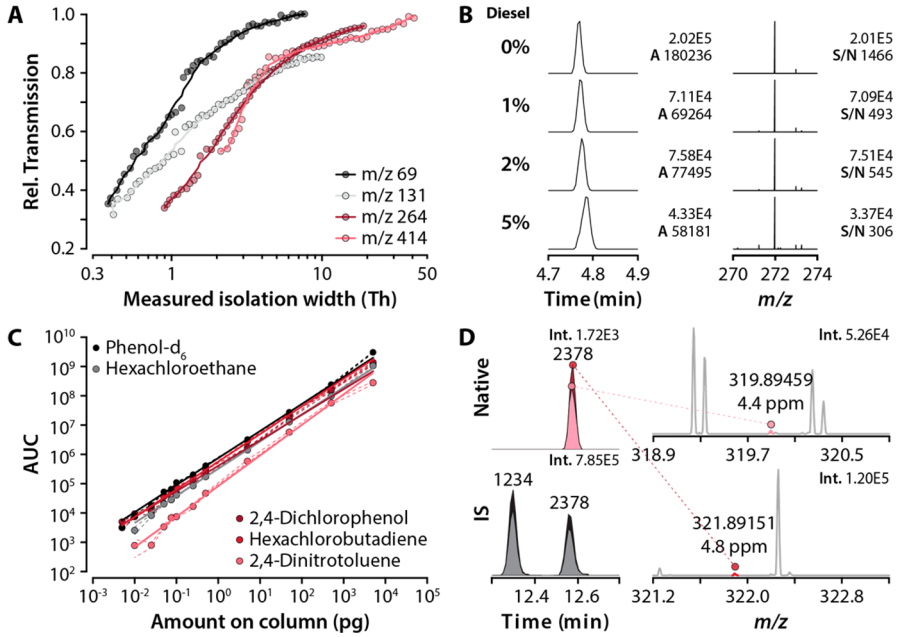

Figure 4. (A) Quadrupole isolation transmission efficiency. Transmission relative to rf-only (q = 0.706) operation is plotted for four stable FC-43 ions as a function of measured isolation width using an AGC target of 1×10^5, 17 500 resolution, and <100 ms injection times. (B) Chromatographic and spectral performance of 1 pg octafluoronaphthalene (OFN) in 0–5% v/v diesel. Chromatographic peak areas (denoted "A") and spectral signal-to-noise (S/N) are noted. (C) Response curves (peak area versus amount on column) for 5 of 94 EPA 8270 compounds targeted by scheduled SIM (3 Th) over 6 orders-of-magnitude. Linearity and detection limit data are given Table 1 and Supplemental Figure S4 in the Supporting Information. (D) Quantification of 2,3,7,8-TCDD at 10–15 fg on column in human pooled blood extract. At left, extracted ion chromatograms (±10 ppm, 5 pt Gaussian smoothing) of native congener quantification isotopomers, m/z 320 and m/z 322, analyzed in separate SIM (4 Th) scans, and of ^{13}C-labeled internal standard (IS) congeners analyzed in full scan are plotted. The single-scan SIM mass spectra at the elution apex for the targeted native congener isotopomers are plotted at right.

Table 1. Linearity, Detection Limit (DL) S/N, and DL Mass Error for SIM Response Curves in Figure 4C and DL Data in Supplemental Figure S4 in the Supporting Information

analyte	slope	adjusted R^2	% RSD	detection limit (pg)	DL S/N[a]	DL mass error (ppm)[b]
phenol-d_6	0.9244	0.9986	24.7	0.005	5.89 ± 0.55	2.02 ± 2.78
hexachloroethane	0.9262	0.9996	23.9	0.010	5.02 ± 2.20	1.73 ± 2.64
2,4-dichlorophenol	0.8719	0.9911	47.9	0.005	10.2 ± 0.83	3.09 ± 0.57
			18.2	0.025	24.0 ± 3.85	4.36 ± 0.74
hexachlorobutadiene	0.9448	0.9985	28.5	0.005	9.22 ± 0.90	2.68 ± 0.78
2,4-dinitrotoluene	1.0443	0.9950	32.6	0.010	3.98 ± 2.46	6.65 ± 0.91

[a]Average detection limit spectral signal-to-noise ratio (±standard deviation) at peak apex. [b]Average detection limit mass error (±standard deviation) at peak apex.

successfully exclude matrix background and accumulate target ion populations in the allotted time, tighter isolation windows are indicated. In practice, a compromise must be reached between the two processes based on the quadrupole's efficiency of target ion transmission. Quadrupole transmission efficiency curves for for the GC/Q-Orbitrap are plotted in Figure 4A for four stable ions from FC-43. Here, the percent transmission relative to rf-only quadrupole transmission (q = 0.706) of each ion was measured as a function of isolation width (from 50 Th, to the minimum width for the device, 0.4 Th). A low ion target of 1×10^5 was employed to prevent space-charge effects in the c-trap, which become more problematic when a small m/z-range of ions are stored. At unit resolution (1 Th isolation width), isolation transmission efficiency is between 35 and 75% relative to rf only. While even higher transmission at smaller isolation widths is always desired, given the specifications of this quadrupole, transmission was determined to be acceptable.

In general, targeted analyses are performed on samples containing high levels of chemical background in which the target analyte is a very small percentage, not on calibrants as used to benchmark quadrupole transmission efficiency above. Figure 4B shows the analysis of 1 pg of OFN neat and in increasingly complex diesel fuel matrixes. In SIM mode with a 5 Th isolation window around the molecular ion of OFN (m/z 272), 1 pg of OFN was detected at all diesel concentrations with spectral S/N exceeding 1400 and 300 at 0% and 5% diesel (v/v), respectively, despite apparent chromatographic disturbances, ionization suppression by matrix ions, and numerous background ions present in the isolation range at 5%. In other experiments where the mass filter was not used (data not shown), no OFN (1 pg) could be detected in the presence of 1% diesel. While the quadrupole mass filter successfully eliminates matrix background falling outside of the isolation window, it is the mass selectivity provided by high mass accuracy and high resolution mass analysis (here, 70 000) that enables the differentiation of the ion of interest, with m/z verified by high mass accuracy, from co-isolated, and therefore co-enriched, background.

dx.doi.org/10.1021/ac5014767 | Anal. Chem. 2014, 86, 10036–10043

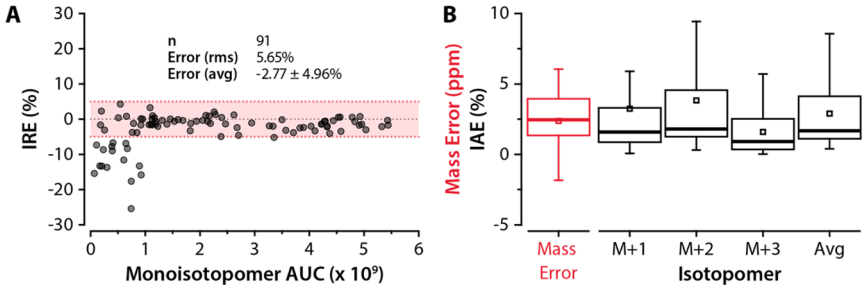

Figure 5. (A) Percent isotopomer ratio error (IRE) versus extracted ion chromatographic peak area for the monoisotopomeric ion (±5 ppm) for 91 of of 94 EPA 8270 compounds in an analysis at 17 500 resolution. Average IRE was −2.77%. (B) Accuracy and precision of mass errors (ppm) and isotopomer abundance errors (IAE, in percent) for 81 putative metabolites and analysis artifacts from the metabolomics study of *Arabidopsis thaliana*. M + 1, M + 2, and M + 3 correspond to the individual IAE for the first, second, and third isotopomers, respectively.

Linear Dynamic Range and Sensitivity. Using a 94 compound EPA 8270[24] mix, linearity, dynamic range, and sensitivity were assessed through replicate injections at amounts ranging from 5 fg to 5 ng, neat, on column, in scheduled targeted-SIM mode. Figure 4C shows response curves for 5 of the 94 compounds. Average linearity (measured as the percent relative standard deviation, % RSD, of response factors, i.e., area-under-the-curve normalized by concentration) was 31.5% RSD, and 26.5% RSD if the 5−10 fg data in the 2,4-dichlorophenol data set were excluded. While the linear regression (adjusted R^2 > 0.99) showed high correlation to a linear model, the moderately high percent RSDs obtained suggest some limitations of the instrument for quantification that need to be further explored. Responses were typically detected down to 5−10 fg on column for chromatographically well-behaved compounds in the mixture. Linearity metrics are presented in Table 1, along with the average peak apex S/N and mass error at the detection limit, i.e., 5 fg on column for phenol-d_6. All compounds in Table 1 were detected at their lowest concentration with greater than S/N 4 and mass errors less than 7 ppm, with little or no chemical interference present in the chromatograms or corresponding spectra (Supplemental Figure S4 in the Supporting Information).

In Figure 4D, we present a further example of the instrument's quantitative performance for toxic, 2,3,7,8-tetrachlorodibenzo-*p*-dioxin (TCDD) and, in Supplemental Figure S5 in the Supporting Information, other polychlorinated dibenzo-*p*-dioxin (CDD) and dibenzofuran (CDF) congeners in a pooled human blood extract matrix. Native 2,3,7,8-TCDD, quantified previously in this sample by magnetic sector MS at ∼10−15 fg/μL, was detected at 10−15 fg on column with low mass errors, and an isotope ratio error (m/z 319/m/z 321) of 8.4%. This meets the EPA 1613 requirement that isotope ratio errors are not greater than 15%.[25] Similarly, isotope ratio errors for native hexa-CDD and hexa-CDF congeners, also at 10−15 fg on column, were −8.3 ± 25% and −29 ± 40% (Supplemental Figure S5 in the Supporting Information). All ^{13}C-labeled congener internal standards were quantified with isotope ratio errors less than 3%. Affirming the linearity and reproducibility of these measurements, we further assessed the intrarun response reproducibility of six TCDD congeners at 10 fg on column, near the limit-of-detection, as 15% (m/z 322) and 21% (m/z 320) RSD with isotope ratio errors of −12 ± 24% (Supplemental Figure S6A in the Supporting Information). With a similar mixture where TCDD congener amounts on column were 2, 5, 10, 25, 50, and 100 fg, intrarun linearity was measured as 15% RSD of response factors from 5 to 100 fg on column (2 fg on column was not detected). Over the detected concentration range, isotopic ratio errors were −4 ± 17% (Supplemental Figure S6B in the Supporting Information).

These data reflect the benefit of quadrupole mass filtering (SIM) in maintaining linearity over a wide dynamic range and extending detection limits. Indeed, these measurements would have not been possible without quadrupole isolation. Additionally, high resolution and accurate mass analysis permitted separation of signals of interest from background signals, even at trace levels in heavy matrix, to maintain isotopic ratio fidelity and mass accuracy. These attributes additionally enable the instrument to meet the analysis requirements of EPA methods, like 1613, normally requiring magnetic sector instrumentation.[25]

Isotopomer Abundance Accuracy. Isotopomer abundances, peak shapes, and/or isotopic fine structure can serve as important orthogonal filters for candidate elemental compositions. Typically, the error of the ratio of the sum of the mono- and first isotopomer abundances over the monoisotopomer abundance,[26] or the error of the relative abundances of the first through third isotopomers,[7] are used to assess isotopomer abundance accuracy. Using the former method in Figure 5A, isotopomer ratio errors (IRE) for 91 of the 94 aforementioned EPA 8270 analytes are plotted as a function of monoisotopomer abundance, extracted at a tolerance of ±5 ppm, in a full scan analysis of 5 ng on column with resolution 17 500. An average error of −2.77 ± 4.96% was observed for all 91 compounds ($error_{rms}$ = 5.65%). Only extracted monoisotopomer peaks with areas less than 1 × 10^9 exhibited isotopomer ratio errors greater than ±5%. Note Orbitrap isotopomer abundance accuracy is inversely related to mass analysis resolution. Thus, analyses using resolutions greater than the 17 500 used here would likely exhibit lower isotopomer abundance accuracy (∼10% at resolution 100 000).[9,27]

These data indicate that the GC/Q-Orbitrap, with the combination of very high mass accuracy, high resolution, and isotopomer abundance errors on average less than 5%, will be a powerful tool for the determination of unique elemental composition for mass spectral features of interest. In the accompanying article,[13] this hypothesis is borne out in the ability to uniquely assign elemental compositions to over 80 putative *Arabidopsis thaliana* metabolites and analysis artifacts. For that set of assignments, the distribution of mass and isotopomer abundance errors are displayed in Figure 5B. Again, isotopomer abundance errors are on average less than 5%, with median errors less than 2.5%. Mass errors average about 2.5 ppm.

dx.doi.org/10.1021/ac5014767 | *Anal. Chem.* 2014, 86, 10036−10043

Tools for Structural Characterization of Unknowns. The GC/Q-Orbitrap also has capabilities for structural elucidation. Identification in GC/MS requires comparison of retention time and fragmentation pattern against authentic, preferably internal, reference standards. For a true unknown, a reasonable structural hypothesis is required to guide the purchase and/or synthesis of potential reference standards. While EI-based full-scan spectra are typically rich with ions from which structural inferences can be made, this process can be prohibitively difficult, especially for low-level analytes or analytes that coelute with other species. As such, alternative analysis modalities can be beneficial to elucidate structure. Numerous such analysis tools have been implemented on the GC/Q-Orbitrap instrument, including alternative ionization types (positive or negative chemical ionization with any reagent gas, e.g., methane, acetonitrile (ACN), isobutane, acetone, etc.), targeted-MS/MS (and targeted-SIM), and advanced data-dependent MS/MS capabilities. Supplemental Figure S7 in the Supporting Information provides examples of these analysis modes, and the accompanying article[13] explores the use of advanced data-dependent MS/MS acquisition in detail.

Figure 6 presents a unifying example of how all of the aforementioned analysis modalities can be used in concert to characterize an unknown, such as a fatty acid methyl ester (FAME) produced from a bacterial source. The EI spectrum of the unknown in Figure 6A has a molecular ion mass of 310.286 63 Th, corresponding to an elemental formula of $C_{20}H_{38}O_2$. While the EI spectrum is indistinguishable from the unknown's cyclic and monoenoic isobars, methyl methylene-octadecanoate (C18:1 CFA) and methyl nonadecenoate (C19:1), the unknown elutes nearly 30 s prior to these isobars.

Following hydrogenation of the bacterial FAME sample, the retention time of the unknown was found to increase, indicating a higher m/z, and yield the EI spectrum in Figure 6B. This spectrum indicates that the unknown is monoenoic, as the molecular ion mass increased to 312.302 28 Th, corresponding to the addition of 2 hydrogens for a hydrogenated composition of $C_{20}H_{40}O_2$. Again distinct in spectrum and retention time from its saturated isobar, nonadecanoate (C19:0), the EI spectrum of the hydrogenated unknown also has characteristic fragment ions that suggest a methyl branch at carbon 11.[28,29] This spectrum matches well with the reference spectrum of methyl 11-methyl-octadecanoate (11-methyl-C18:0). From this information, the unknown can be said to possess the general structure of methyl 11-methyl-octadecenoate (11-methyl-C18:1), although the location of the double bond remains unknown.

To localize the double bond, ACN PCI was next employed. In ACN PCI, the reactive species generated by self-ionization of ACN, 1-methyleneimino-1-ethyenylium (MIE) or $H_2C{=}N^+{=}C{=}CH_2$, covalently adducts to the double bonds of unsaturated FAMEs to produce a distinct ion, corresponding to $[M + MIE]^+$, in the MS spectrum. Isolation and collisional dissociation of the $[M + MIE]^+$ ion results in diagnostic fragment ions that permit unambiguous localization of double bonds within the FAME.[30−33] The ACN PCI MS spectrum, in the top panel of Figure 6C, shows the $[M + MIE]^+$ ion of the unknown at m/z 364.321 01 with elemental composition, $C_{23}H_{42}O_2N$. Targeted MS/MS of this ion reveals diagnostic α and ω ions that correspond to fragmentation allylic to the double bond (plus a transferred proton). These ions successfully localize the double bond to position 12. Thus, the structure of the unknown can be tentatively assigned as

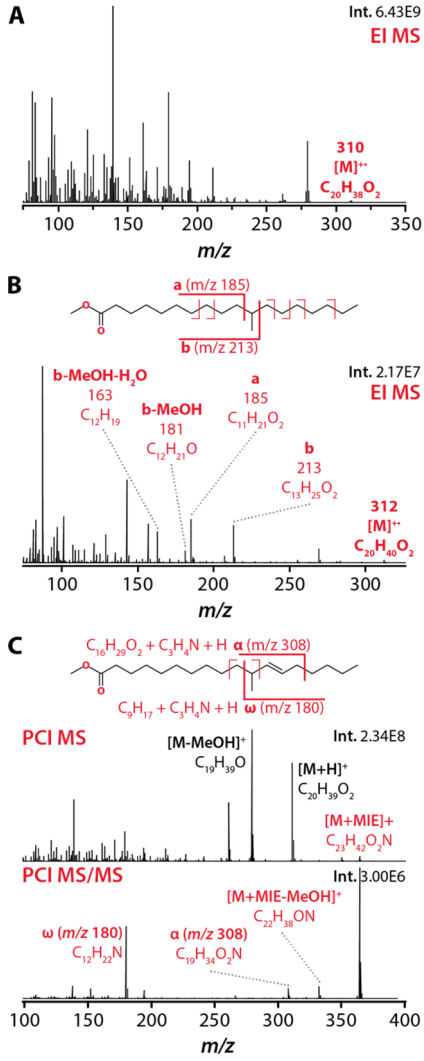

Figure 6. Identification of an unknown fatty acid methyl ester. (A) EI mass spectrum of the untreated unknown. (B) EI mass spectrum of the unknown following hydrogenation, indicating that the unknown is monoenoic (2 Th mass shift with hydrogenation), and has a branched structure based on characteristic fragments a and b. The proposed structure of the hydrogenated unknown is depicted above. (C) Acetonitrile PCI MS and MS/MS spectra. The MS spectrum shows several molecular ion adducts, including $[M + MIE]^+$. The $[M + MIE]^+$ ion was isolated and fragmented at 25 eV to generate the MS/MS spectrum. The characteristic α and ω ions localize the double bond. The proposed structure of the unknown is shown above.

methyl 11-methyl-12-octadecenoate (11-methyl-12-C18:1). While synthesis and side-by-side analysis of this compound is required to confirm this assignment, this vignette demonstrates, using a combination of EI, ACN PCI, full scan MS, and targeted MS/MS, the flexibility of the GC/Q-Orbitrap to resolve intractable structural characterization and identification challenges.

CONCLUSION

We have described the construction, optimization, and evaluation of a new high-resolution GC/MS, the GC/Quadrupole-Orbitrap. This benchtop instrument is the first-ever, applications-grade, Orbitrap-based instrument dedicated for GC/MS. The GC/Quadrupole-Orbitrap robustly generates, transmits, manipulates, and detects EI/CI-generated ions

dx.doi.org/10.1021/ac5014767 | Anal. Chem. 2014, 86, 10036−10043

supplied by a GC in four modes: full scan, SIM with quadrupole isolation, "all ion fragmentation"-MS/MS with beam-type CAD in the HCD collision cell, and MS/MS with both quadrupole isolation and beam-type CAD. With a dynamic, parallelized ion injection and mass analysis scheme with AGC, this instrument boasts a 23 Hz (32 ms transient) scan rate at resolution 10 000 (at m/z 200), and a 1 Hz scan rate at resolution 200 000, all while maintaining low-to-subppm mass errors. Use of the quadrupole mass filter enables low-femtogram detection limits for common pollutants, with a linear dynamic range spanning 6 orders-of-magnitude. Lastly, the high signal-to-noise, high mass accuracy, and high resolution data generated by this instrument facilitate annotation of unknown spectral features with chemical formulas and enable structural characterization through flexible analysis modalities.

The GC/Q-Orbitrap has potential to increase the rate of success for annotation and identifications of unknowns in the analysis of complex biological or environmental samples. By enabling researchers in diverse fields to come closer to the full story in their GC/MS analyses, the GC/Q-Orbitrap has promise to bridge the fundamental technology gap in accurate mass and high-resolution instrumentation that exists today in small molecule analysis.

■ ASSOCIATED CONTENT

Supporting Information

Additional figures and tables. This material is available free of charge via the Internet at http://pubs.acs.org.

■ AUTHOR INFORMATION

Corresponding Author

*Phone 608-263-1718. Fax: 608-890-0167. E-mail: jcoon@chem.wisc.edu.

Notes

The authors declare no competing financial interest.

■ ACKNOWLEDGMENTS

We thank A.J. Bureta for illustration support and colleagues at Thermo Fisher Scientific, especially Eduard Denisov, Alexander Makarov, Frank Czemper, John E. P. Syka, and Jae Schwartz, for helpful discussions and feedback. *Arabidopsis thaliana* samples were kindly provided by Benjamin B. Minkoff and Prof. Michael R. Sussman (UW-Madison, Dept. of Biochemistry). This work was funded by Thermo Fisher Scientific, the National Institutes of Health (Grant 1R01GM107199), and the Department of Energy, Office of Science, Great Lakes Bioenergy Research Center (Grant DC-FC02-07ER64494).

■ REFERENCES

(1) Fiehn, O. *TrAC, Trends Anal Chem.* **2008**, *27*, 261−269.
(2) Fiehn, O.; Kopka, J.; Dormann, P.; Altmann, T.; Trethewey, R. N.; Willmitzer, L. *Nat. Biotechnol.* **2000**, *18*, 1157−1161.
(3) Fiehn, O.; Kopka, J.; Trethewey, R. N.; Willmitzer, L. *Anal. Chem.* **2000**, *72*, 3573−3580.
(4) Kumari, S.; Stevens, D.; Kind, T.; Denkert, C.; Fiehn, O. *Anal. Chem.* **2011**, *83*, 5895−5902.
(5) Kim, S.; Rodgers, R. P.; Marshall, A. G. *Int. J. Mass Spectrom.* **2006**, *251*, 260−265.
(6) Kind, T.; Fiehn, O. *BMC Bioinf.* **2006**, *7*, 234.
(7) Kind, T.; Fiehn, O. *BMC Bioinf.* **2007**, *8*, 105.
(8) McAlister, G. C.; Berggren, W. T.; Griep-Raming, J.; Horning, S.; Makarov, A.; Phanstiel, D.; Stafford, G.; Swaney, D. L.; Syka, J. E. P.; Zabrouskov, V.; Coon, J. J. *J. Proteome Res.* **2008**, *7*, 3127−3136.
(9) Peterson, A. C.; McAlister, G. C.; Quarmby, S. T.; Griep-Raming, J.; Coon, J. J. *Anal. Chem.* **2010**, *82*, 8618−8628.
(10) Kind, T.; Fiehn, O. *Bioanal Rev.* **2010**, *2*, 23−60.
(11) Geiger, T.; Cox, J.; Mann, M. *Mol. Cell. Proteomics* **2010**, *9*, 2252−2261.
(12) Michalski, A.; Damoc, E.; Hauschild, J. P.; Lange, O.; Wieghaus, A.; Makarov, A.; Nagaraj, N.; Cox, J.; Mann, M.; Horning, S. *Mol. Cell. Proteomics* **2011**, *10*, 1−11.
(13) Peterson, A. C.; Balloon, A. J.; Westphall, M. S.; Coon, J. J. *Anal. Chem.* **2014**, DOI: 10.1021/ac5014755.
(14) Olsen, J. V.; Schwartz, J. C.; Griep-Raming, J.; Nielsen, M. L.; Damoc, E.; Denisov, E.; Lange, O.; Remes, P.; Taylor, D.; Splendore, M.; Wouters, E. R.; Senko, M.; Makarov, A.; Mann, M.; Horning, S. *Mol. Cell. Proteomics* **2009**, *8*, 2759−2769.
(15) Second, T. P.; Blethrow, J. D.; Schwartz, J. C.; Merrihew, G. E.; MacCoss, M. J.; Swaney, D. L.; Russell, J. D.; Coon, J. J.; Zabrouskov, V. *Anal. Chem.* **2009**, *81*, 7757−7765.
(16) Michalski, A.; Damoc, E.; Lange, O.; Denisov, E.; Nolting, D.; Mueller, M.; Viner, R.; Schwartz, J.; Remes, P.; Belford, M.; Dunyach, J.-J.; Cox, J.; Horning, S.; Mann, M.; Makarov, A. *Mol. Cell. Proteomics* **2011**, *11*, 1−11.
(17) Lange, O.; Damoc, E.; Wieghaus, A.; Makarov, A. In *Proceedings of the 59th Conference of the American Society of Mass Spectrometry and Allied Topics*, Denver, CO, 2011.
(18) Lange, O.; Makarov, A.; Denisov, E.; Balschun, W. In *Proceedings of the 58th Conference of the American Society Mass Spectrometry*, Salt Lake City, UT, 2010.
(19) Makarov, A. In *Proceedings of the 58th Conference of the American Socety of Mass Spectrometry*, Salt Lake City, UT, 2010.
(20) Montanari, C.; Sado Kamdem, S. L.; Serrazanetti, D. I.; Etoa, F.-X.; Guerzoni, M. E. *Food Microbiol.* **2010**, *27*, 493−502.
(21) Fiehn, O. In *Arabidopsis Protocols*, 2nd ed.; Salinas, J., Sanchez-Serrano, J. J., Eds.; Humana Press: Totowa, NJ, 2006; Vol. *323*; 439−447.
(22) NIST. *NIST/EPA/NIH Mass Spectral Library and NIST GC Retention Index Database*, 2011.
(23) Dawson, P. H. *Quadrupole Mass Spectrometry and its Application*; Elsevier Scientific Publishing Co: New York, 1976.
(24) EPA. *EPA Method 8270C: Semivolatile Organic Compounds by Gas Chromatography/Mass Spectrometry (GC/MS)*, 1996; pp 1−54.
(25) EPA. *EPA Method 1613: Tetra- through Octa-Chlorinated Dioxins and Furans by Isotope Dilution HRGC/HRMS*, 1994; pp 1−86.
(26) Abate, S.; Ahn, Y. G.; Kind, T.; Cataldi, T. R. I.; Fiehn, O. *Rapid Commun. Mass Spectrom.* **2010**, *24*, 1172−1180.
(27) Erve, J. C. L.; Gu, M.; Wang, Y.; DeMaio, W.; Talaat, R. E. *J. Am. Soc. Mass Spectrom.* **2009**, *20*, 2058−2069.
(28) Apon, J. M. B.; Nicolaides, N. *J. Chromatogr. Sci.* **1975**, *13*, 467−473.
(29) Ryhage, R.; Stenhagen, E. *Ark. Kemi* **1960**, *15*, 291−304.
(30) Van Pelt, C. K.; Brenna, J. T. *Anal. Chem.* **1999**, *71*, 1981−1989.
(31) Oldham, N. J.; Svatos, A. *Rapid Commun. Mass Spectrom.* **1999**, *13*, 331−336.
(32) Michaud, A. L.; Diau, G. Y.; Abril, R.; Brenna, J. T. *Anal. Biochem.* **2002**, *307*, 348−360.
(33) Michaud, A. L.; Yurawecz, M. P.; Delmonte, P.; Corl, B. A.; Bauman, D. E.; Brenna, J. T. *Anal. Chem.* **2003**, *75*, 4925−4930.